STRUCTURAL BIOLOGY

The mechanism of Hsp90-induced oligomerizaton of Tau

S. Weickert[1,2]*, M. Wawrzyniuk[3]*†, L. H. John[1]‡, S. G. D. Rüdiger[3]§, M. Drescher[1,2]§

Aggregation of the microtubule-associated protein Tau is a hallmark of Alzheimer's disease with Tau oligomers suspected as the most toxic agent. Tau is a client of the molecular chaperone Hsp90, although it is unclear whether and how the chaperone massages the structure of intrinsically disordered Tau. Using electron paramagnetic resonance, we extract structural information from the very broad conformational ensemble of Tau: Tau in solution is highly dynamic and polymorphic, although "paper clip"–shaped by long-range contacts. Interaction with Hsp90 promotes an open Tau conformation, which we identify as the molecular basis for the formation of small Tau oligomers by exposure of the aggregation-prone repeat domain to other Tau molecules. At the same time, formation of Tau fibrils is inhibited. We therefore provide the nanometer-scale zoom into chaperoning an amyloid client, highlighting formation of oligomers as the consequence of this biologically relevant interaction.

INTRODUCTION

Tau is an intrinsically disordered protein (IDP) known to bind to and stabilize microtubules (MTs) and regulate axonal transport in its physiological function (1–3). In pathology, filamentous aggregates of Tau constitute a hallmark of neurodegenerative diseases, among them Alzheimer's disease (AD) (4). Both MT binding and self-aggregation of Tau are mediated by the Tau repeat domain (Tau-RD) consisting of four imperfect repeats in the longest Tau isoform (Fig. 1A) (5, 6).

While Tau in solution is generally disordered and highly dynamic, long-range interactions mediate folding back of both termini onto Tau-RD, resulting in an overall "paper-clip" arrangement of monomeric Tau, which has been well established by a variety of experimental techniques such as nuclear magnetic resonance (NMR) and fluorescence resonance energy transfer (FRET) (7, 8). In filamentous aggregates of Tau, Tau-RD forms the ordered filamental core, while N- and C-terminal regions remain a disordered "fuzzy coat" (9, 10). Tau filaments exist in different morphologies with notable differences in the fold of the filamental cores, which are probably disease specific (11, 12). Although fibrils have long been considered the neurotoxic species, neuronal death appears rather to be caused by prefibrillar soluble aggregates and oligomers of Tau (13, 14), which are also considered responsible for spreading Tau pathogenicity from cell to cell in a prion-like concept (15, 16).

The molecular chaperone heat shock protein 90 (Hsp90) (17, 18) initiates proteasomal degradation (19–21) and induces oligomerization of Tau (22–24). Tau-RD is part of the Hsp90/Tau interaction interface (25). While insight into the molecular mechanism of the emergence of toxic Tau oligomers is highly relevant in the context of neuropathology, its structural principle is elusive.

The lack of a defined three-dimensional fold of IDPs like Tau makes their structural characterization challenging. Electron para-magnetic resonance (EPR) spectroscopy in combination with site-directed spin labeling has proven powerful in the investigation of IDPs and their aggregation behavior also in the presence of diverse interaction partners (26–31). EPR spectroscopy (i) provides information about the side-chain dynamics of a single residue (32). Dipolar spectroscopy, i.e., DEER (double electron-electron resonance) spectroscopy, (ii) gives access to distance information in the nanometer range between two spin labels by measuring their magnetic dipolar interaction frequency ω_{dd} (33–35). Here, we exploit the combination of these approaches to investigating the molecular mechanism of Hsp90-induced Tau oligomerization.

RESULTS

We genetically engineered Tau derivatives containing one or two cysteines at specific sites and performed thiol-specific spin labeling (Fig. 1B). A range of biochemical and biophysical assays was used to monitor the success of the labeling reaction and the structural integrity of the protein (figs. S1 to S3 and table S1).

Next, we set out to characterize the structural properties of Tau by obtaining long-range intramolecular distance information with DEER on doubly spin-labeled Tau. Typical experimental DEER form factors for Tau are shown in Fig. 1C (full data in fig. S4) in comparison to simulated data for a hypothetical, well-defined distance. In contrast to the latter, the experimental traces for Tau showed no distinct modulations, indicating a broad distribution of spin-spin distances and thus implying a vast conformational ensemble of Tau in solution.

For these experimental DEER traces, the standard method for DEER data analysis fails, and the extraction of precise distance distributions is precluded (36, 37). First, we tested whether the experimental DEER data are in agreement with a simple random coil (RC) model (fig. S5). We chose RC model parameters as published by Rhoades and co-workers (38, 39) for assessing the results of FRET experiments on Tau. For certain spin-labeled stretches of Tau, e.g., Tau-17*-103*, the RC model agreed well with the experimental results (Fig. 1D and fig. S5), indicating an RC-like structural ensemble in the corresponding Tau segments. However, the RC model cannot describe the whole DEER dataset even taking variation of RC parameters depending on solvent quality into account [see fig. S6; (40, 41)]: For Tau-17*-291* and Tau-17*-433*, the deviation between the experiment and the RC model indicates a considerable

[1]Department of Chemistry, University of Konstanz, 78457 Konstanz, Germany. [2]Konstanz Research School Chemical Biology (KoRS-CB), University of Konstanz, 78457 Konstanz, Germany. [3]Cellular Protein Chemistry, Bijvoet Center for Biomolecular Research, Utrecht University, Padualaan 8, 3584 CH Utrecht, Netherlands.
*These authors contributed equally to this work.
†Present address: Department of Infectious Diseases and Immunology, Utrecht University, Yalelaan 1, 3584CL Utrecht, Netherlands.
‡Present address: Department of Biochemistry, University of Oxford, Oxford OX1 3QU, UK.
§Corresponding author. Email: s.g.d.rudiger@uu.nl (S.G.D.R.); malte.drescher@uni-konstanz.de (M.D.)
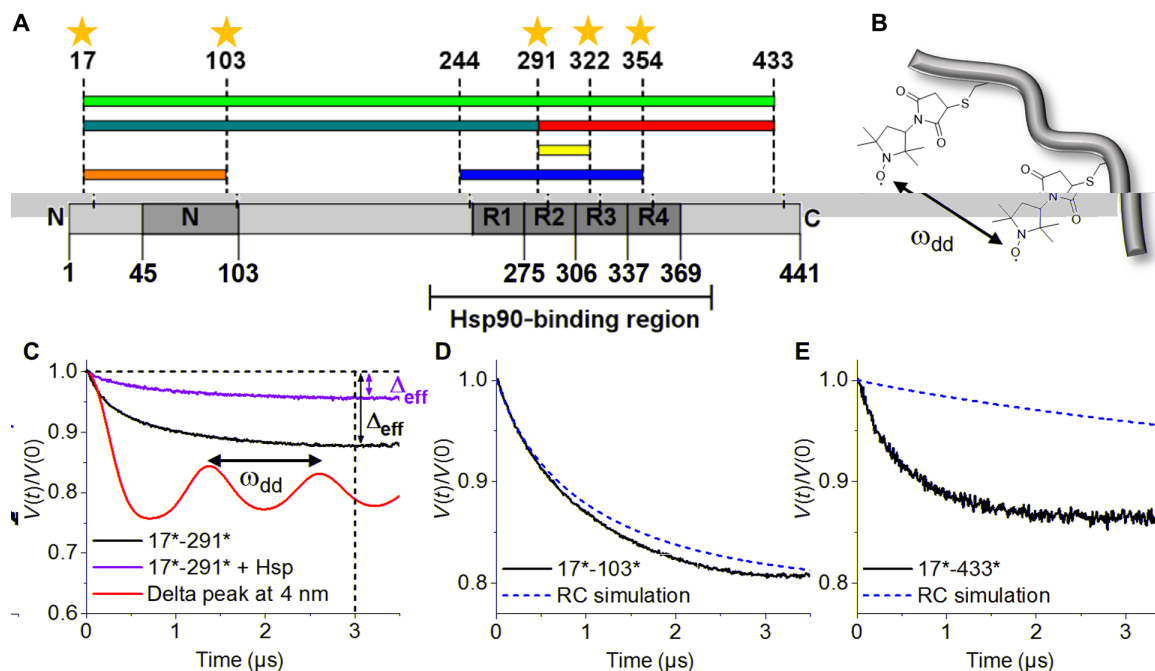
Fig. 1. DEER with modulation depth–based data analysis allows monitoring the conformational ensemble of Tau. (**A**) Tau domain organization (R1 to R4, pseudorepeats; N, two N-terminal inserts). Stars indicate labeling positions in singly spin-labeled Tau derivatives. Colored bars depict sequences spanned by labels in doubly spin-labeled Tau. (**B**) 3-Maleimido proxyl spin label side chains attached to cysteines. (**C**) Modulations with the dipolar modulation frequency ω_{dd} characterize a DEER time trace calculated for a delta peak at 4 nm (green). Experimental intramolecular DEER time traces recorded for Tau-17*-291* are modulation free in the absence (black) and presence (orange) of Hsp90 indicating broad distributions of ω_{dd} and thus a broad conformational ensemble. Effective modulation depths Δ_{eff} at $t = 3$ μs provide information about the Tau conformational ensemble without or with Hsp90. (**D**) A random coil (RC) model is in reasonable agreement with DEER results for several labeled stretches of Tau, e.g., Tau-17*-103*. (**E**) Experimental results, e.g., for Tau-17*-433* suggest a considerably larger vicinity of spin labels than the RC simulation predicts, consistent with a paper-clip solution ensemble of Tau.
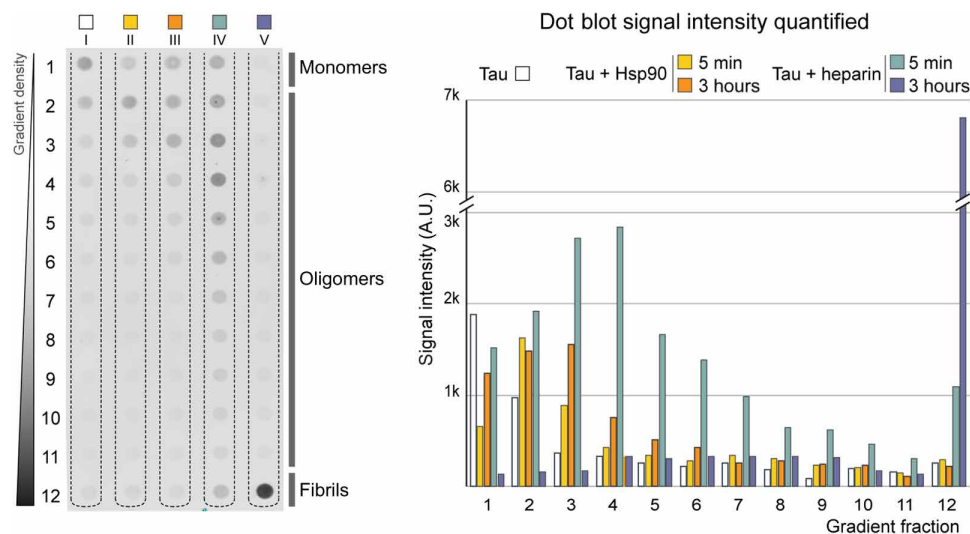

Fig. 2. Hsp90 promotes the formation of small oligomeric species of Tau. Dot blot summarizing the results of density gradient centrifugation and quantification (the color code represents Tau preparations as reported on top of the right graph): Pure Tau is mostly monomeric. Heparin induces formation of high–molecular weight fibrils. Hsp90 leads to an increase in small Tau oligomeric species, while formation of fibrils is prohibited. A.U., arbitrary units.

contribution from Tau conformations more compact than RC (Fig. 1E and fig. S5). This is in good agreement with the well-established finding that Tau does not adopt RC conformation in solution but rather a paper clip (7, 8).

Hinderberger and co-workers (36, 37) proposed a data analysis procedure, which we adapted for analyzing the broad conformational ensemble of a large IDP like Tau. We evaluated the DEER data using the effective modulation depth Δ_{eff}, which is the signal decay of the
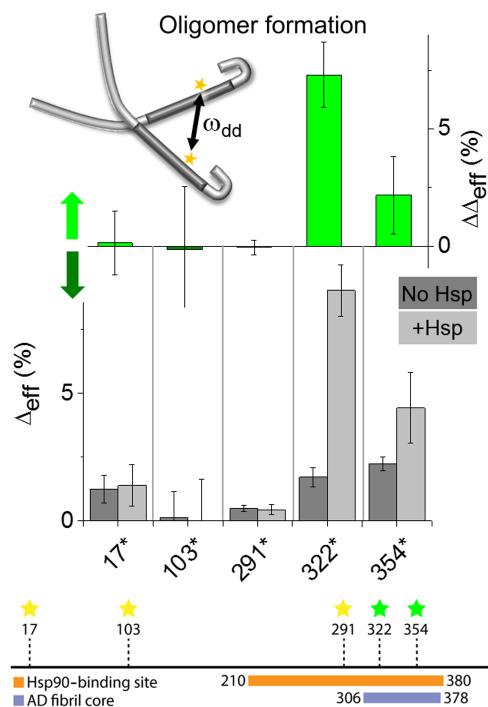
Fig. 3. Oligomerization is mediated by the AD fibril core region of Tau. Information about intermolecular Tau/Tau interactions obtained with DEER of singly spin-labeled Tau in the absence (dark gray) and presence (light gray) of Hsp90. Nonzero Δ_{eff} values represent small amounts of nonmonomeric Tau in the absence of Hsp90. Hsp90 increased Δ_{eff} values for Tau-322* and Tau-354* (light green bars) in accordance with an increase in Tau oligomers mediated by R3/R4 of Tau-RD. Positions probed in the experiment are also indicated on a schematic representation of the Tau sequence, with indicated Hsp90-binding site (25) and the core of the AD fibril (11), yellow and green stars indicating spin labeling positions without and with changes in Δ_{eff} upon addition of Hsp90, respectively.

DEER time trace at time t = 3 μs (Fig. 1C). While a DEER trace in the absence of Hsp90 delivers a reference Δ_{eff} value for each Tau sample, the change $\Delta\Delta_{eff}$ upon addition of Hsp90 characterizes transitions in the conformational equilibrium: Negative $\Delta\Delta_{eff}$ values indicate an increase in spin-spin separation, while positive Δ_{eff} values are consistent with the spins coming into closer proximity of each other (see details of modulation depth–based approach in fig. S7). This allows extracting distance information from DEER traces not analyzable in the conventional way.

The systematic analysis of the experimental Δ_{eff} values supports the paper-clip model proposed on the basis of FRET and NMR experiments for Tau in solution, where N and C termini are in proximity to each other, and Tau-RD is in an overall more compact fold than RC (7, 8). On the one hand, these results demonstrate the capacity of the Δ_{eff} approach for obtaining structural information from DEER traces reflecting vast protein ensembles, while on the other hand, they define the paper clip as a reference structural ensemble of Tau in solution, which is in agreement with the results obtained for the Tau structural ensemble in previous studies, suggesting a paper clip or S shape in solution (7, 8, 39, 42).

It has been shown that Hsp90 induces oligomerization of Tau fragments (22). Here, we analyzed the oligomerization behavior of full-length Tau by density gradient centrifugation (Fig. 2). Pure Tau was mainly found in its monomeric form, while heparin induced the

formation of mature fibrils. In the presence of Hsp90, the amount of small oligomeric Tau species increased. Notably, the formation of high–molecular weight Tau aggregates and fibrils was prevented in the presence of Hsp90. Electron micrographs of K18 Tau fragments in the presence of Hsp90 also show the formation of small protein conglomerates, while fibril formation is prevented (43).

To identify the oligomerization domain in Tau relevant for Hsp90-induced oligomerization, we performed intermolecular DEER measurements using singly spin-labeled Tau: Upon oligomerization, Δ_{eff} would increase locally where inter-Tau contacts are established. We observed very small Δ_{eff} values for all Tau derivatives in the absence of Hsp90 (Fig. 3), indicating only minor subpopulations of oligomeric Tau species. Addition of Hsp90 leads to a considerable increase in Δ_{eff} for Tau-322* and Tau-354*, depicted as difference values $\Delta\Delta_{eff}$. This suggests that the oligomerization interface is located in Tau-RD and specifically in R3/R4. Notably, Tau oligomerization initiates in the same Tau region responsible for AD fibril formation and Hsp90 binding (11, 25). This is remarkable, as it suggests that the same stretch of Tau mediating fibril formation (25) is addressed by Hsp90 to promote the formation of oligomers.

The dynamic properties of Tau in solution and with Hsp90 are reported by EPR spectra of spin-labeled Tau side chains. In general, we observed rather fast rotational dynamics with rotational correlation times τ_{corr} around 1 ns (Fig. 4A). This is in accordance with Tau presiding in a largely unstructured state with a broad conformational ensemble and a high degree of dynamical disorder (26). Addition of Hsp90 induced only subtle changes in the spectra (fig. S9), indicating that dynamic disorder in Tau persists also when bound. The generally still fast dynamics in the Tau spectra hints toward a transient nature of the Tau/Hsp90 complex, as only a small portion of spin-labeled Tau might be motionally restricted by intermolecular contacts, while other Tau molecules retain unrestricted rotational diffusion. We determined the half lifetime of the Tau/Hsp90 complex by quartz crystal microbalance (QCM) affinity measurements at ~10 s, which is typical for transient protein-protein interactions (fig. S10 and table S2) (44). The Tau/Hsp90 complex appears to be characterized by transient interactions between individual residues, involving a structural multiplicity of Tau.

We observed local restrictions of the reorientational mobility for spin-labeled side chains Tau-291* and Tau-322* in the presence of Hsp90. Both residues are located in Tau-RD, which has been identified as the Hsp90-binding region before (25). Thus, the altered dynamics are attributed to direct Tau/Hsp90 interaction, while also oligomer formation might restrict side chain dynamics of Tau-322*.

Spin label mobilities increased in Tau-17* and Tau-103* upon addition of Hsp90, indicating that these side chains gain a larger conformational space. Thus, one might speculate that the N terminus detaches from Tau-RD upon binding of Hsp90, opening up the paper-clip fold.

To elucidate the structural influence of Hsp90 on the Tau conformational ensemble, we performed DEER spectroscopy of doubly spin-labeled Tau. DEER traces remained modulation free upon addition of Hsp90 (fig. S4). Thus, dynamic disorder prevails in Tau also when interacting with the chaperone (Fig. 1C). Addition of Hsp90 changed Δ_{eff} values, indicating a shift in the conformational equilibrium of Tau (Fig. 4B): A pronounced increase in the average spin-spin separation occurred for Tau-17*-291* and Tau-17*-433*. This indicates that the N terminus detaches from both Tau-RD and the C terminus and folds outward, opening up the paper clip (Fig. 5).
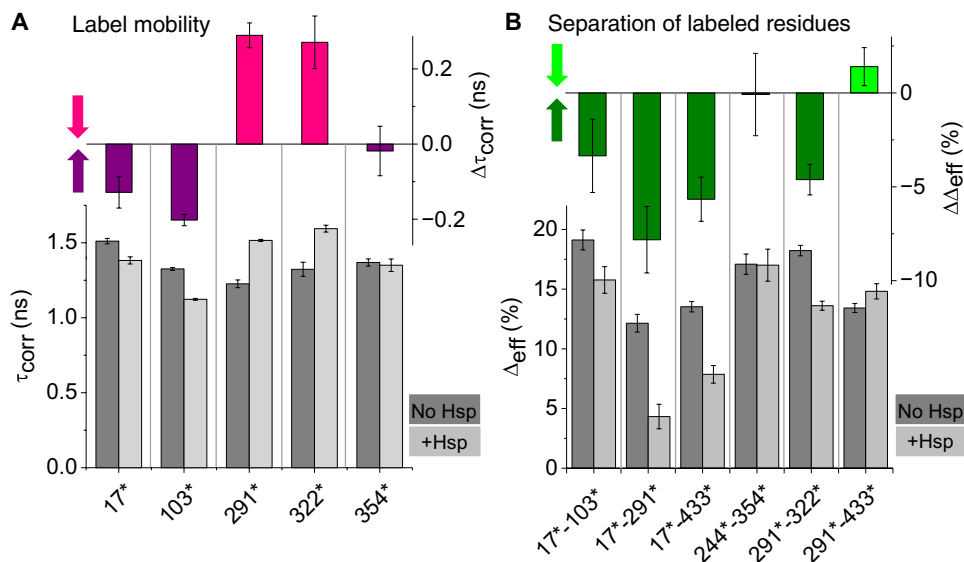
Fig. 4. EPR of singly and doubly spin-labeled Tau derivatives gives access to Tau side-chain dynamics and intramolecular distance information. (**A**) Local side-chain dynamics accessed by cw EPR of 28 μM singly spin-labeled Tau derivatives: Rotational correlation times τ_{corr} determined in the absence (dark gray) and presence (light gray) of 56 μM Hsp90 and respective changes $\Delta\tau_{corr}$ (purple/pink) are shown. Arrows indicate a decrease (pink) or increase (purple) in side-chain mobility at the respective site. (**B**) Intramolecular distance information obtained by DEER spectroscopy with doubly spin-labeled Tau derivatives: Effective modulation depths Δ_{eff} determined in the absence (dark gray) and presence (light gray) of Hsp90 and respective changes $\Delta\Delta_{eff}$ (light/dark green) are shown. Arrows indicate a decrease (light green) or increase (dark green) in spin label separation.
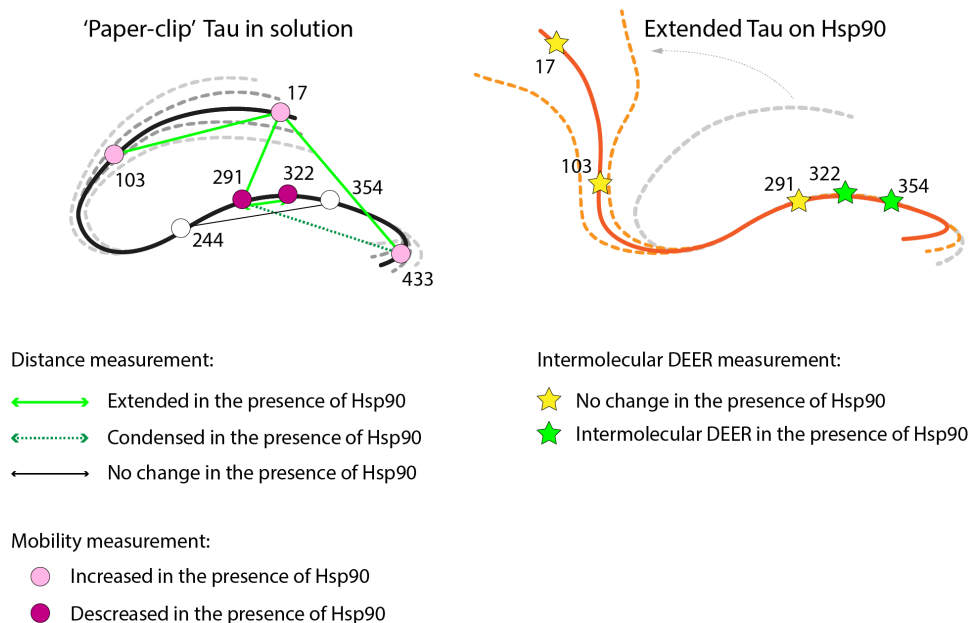

Fig. 5. Binding to Hsp90 induces a conformational opening of 'paper-clip' Tau. A structural model of Tau in the absence (left) and presence of Hsp90 (right) can be derived from EPR data of the Tau conformational ensemble. In the absence of Hsp90, Tau adopts a paper-clip shape with both termini folded back onto Tau-RD. In the presence of Hsp90 the N terminus folds outward, thereby uncovering Tau-RD.

$\Delta\Delta_{eff}$ values suggested a slight stretching of N-terminal Tau between Tau-17*-103* and of Tau-RD in the region between Tau-291*-322* in R2/R3, while the overall dimension of Tau-RD between Tau-244*-354* remained unchanged. While individual repeat sequences, e.g., R2/R3 expanded while accommodating Hsp90, there seems to

be considerable flexibility in the remaining Tau-RD for preserving its overall dimension. A similar structural reorganization of Tau toward an open conformation was reported upon binding to tubulin, where stretches between individual repeats expanded, while the overall dimension of Tau-RD remained unaffected (*38*). Our results

report the conformational basis of Tau oligomerization in the presence of Hsp90 and suggest that binding to Hsp90 opens the compact Tau solution structure, exposing Tau-RD residues and presenting them to other Tau molecules. As the Tau/Hsp90 complex is of a transient nature, oligomerization of Tau molecules may then occur via exposed Tau-RD.

DISCUSSION

With a combination of magnetic resonance experiments and biochemical assays, we gained detailed insight into the conformational ensemble of the IDP Tau in the presence of the molecular chaperone Hsp90. While DEER spectroscopy is routinely used to extract distance restraints in well-ordered proteins or small segments of disordered proteins, we demonstrated in the current study how DEER in combination with a pragmatic approach to data analysis can be profitably used in obtaining structural information from a highly polymorphic and dynamic conformational ensemble of a large, full-length IDP. While the structural resolution of our approach is low, it enabled us to shed light on the mechanism of the full-length Tau/Hsp90 interaction on a molecular level.

Probing Tau conformation in solution revealed a paper-clip arrangement of the domains: Fig. 5 shows a structural model of Tau summarizing our findings. The sketch is not an accurate model of Tau structure but an attempt to unite the most relevant results of this study in one possible Tau molecule representing the whole conformational ensemble. The N-terminal domain forms long-range interactions with the aggregation-prone domain, in line with previous findings (22–24). The flexible N terminus may, therefore, preclude aberrant Tau/Tau interactions, resulting in the high solubility of the full-length protein. Tau fragments lacking the N-terminal region, and therefore exposing the aggregation-prone repeat region, feature markedly accelerated aggregation rates, such as Tau-RD (45). Tau-RD is less soluble than the full-length protein despite having a higher net charge (isoelectric point pI 9.67 for Tau-RD versus 8.24 for full length) (45, 46). Hsp90 binds to Tau-RD, consistent with previous findings by us (25). The Tau/Hsp90 complex is distinguished by transient protein-protein interactions with Tau remaining conformationally heterogeneous and dynamically disordered, which is characteristic for "fuzzy" complexes (47, 48) and was also described for a ternary complex of Hsp90 with the *cis–trans* peptidyl-prolyl isomerase (PPIase) FKBP51 (FK506-binding protein of 51 kDa) and Tau complex (49). In the light of the large extension of the Tau/Hsp90 interaction interface (25), it is consistent that single residues contribute only little to the overall binding between Hsp90 and Tau, enabling a high rate of unbinding (47, 48). This is a typical way for Hsp90 to bind its client proteins (50, 51). In addition, Tau typically retains a high degree of conformational dynamics, at least for protein segments, when in complex with various interaction partners including heparin, tubulin, and MTs and in Tau fibrils (9, 26, 38, 52, 53). Binding to Hsp90 induces a conformational opening of paper clip–Tau (7, 8), leading to exposure of Tau-RD.

Hsp90 binding does not alter the global dimension of Tau-RD, similar as Tau bound to tubulin (40). Heparin, in contrast, compacts Tau-RD (39, 54). This suggests that Hsp90 stabilizes Tau in a conformation different from the heparin-induced aggregation-prone one but similar to a conformation that might enable productive binding to MTs (19). It remains to be seen whether the Hsp90-bound shape may be similar to the fibril structure in AD. Hsp90-seeded oligomers exhibit an intermolecular DEER signal solely for the variants sampling the two C-terminal repeats R3 and R4 (Fig. 3) that mediate the early steps of Tau aggregation (26) and eventually constitute the core of the paired helical filament of AD (6, 11). In particular, the position 291 located within the Hsp90-binding region, but not the amyloid core, does not indicate any close Tau/Tau interaction. This hints toward a conclusion that the Tau/Hsp90 interaction promotes self-aggregation after opening the compact Tau solution structure, probably due to exposure of the aggregation-prone Tau-RD. However, the continuation to fibril formation is blocked in the presence of Hsp90, which may foster the generation of Tau oligomers. The conformational transition and opening up of Tau are therefore the structural basis for subsequent formation of deleterious oligomers in the presence of Hsp90.

MATERIALS AND METHODS
Study design
This in vitro EPR study was performed using full-length Tau in the absence and presence of Hsp90. Spin labeling sites were established before in single-molecule FRET (38, 39). Analysis of the conformational ensemble of Tau was based on EPR dipolar spectroscopy using DEER (33–35). Long-range intramolecular distance information was obtained with doubly spin-labeled Tau molecules and supported by monitoring the local side-chain dynamics of singly spin-labeled Tau. In addition, intermolecular interactions were monitored by DEER and singly spin-labeled Tau derivatives to gain insight into the oligomerization state of Tau. Biochemical assays, e.g., sucrose gradient ultracentrifugation, and QCM helped to shape and support the findings.

Protein purification and spin labeling
Human Hsp90b (Uniprot identifyer P08238) and human Tau Isoform F (Uniprot identifyer P10636-8) were prepared as described before (25, 55). Purification protocols and spin labelling procedures are detailed in the Supplementary Materials.

EPR experiments
Samples were prepared with deuterated sample buffer and had final Tau concentrations of 28 μM. Hsp90 was added where applicable at a concentration of 56 μM. For measurements at cryogenic temperatures upon shock freezing, 20% (v/v) [D_8]glycerol was added to the samples.

All continuous wave EPR spectra were recorded at X-band frequency at 293 K on singly spin-labeled Tau derivatives with a typical sample volume of 10 μl. The spectra were analyzed using homewritten MATLAB scripts. Rotational correlation times τ_{corr} were obtained using Kivelson's equation (56).

DEER measurements were performed at Q-band frequency at 50 K with a sample volume of 12.5 μl. DEER raw data were analyzed globally using the DD (Version 7B) software package for MATLAB (57, 58). Effective modulation depths Δ_{eff} were determined as a measure for the effective spin-spin separation as established by Hinderberger and co-workers (36, 37).

Sucrose gradient ultracentrifugation and dot blot
The oligomerization state of Tau samples incubated with Hsp90 or heparin for various incubation times as indicated in Fig. 2 were

resolved by ultracentrifugation on sucrose density gradients. Density gradients were divided into 12 equal fractions of increasing density and subjected to dot blot analysis using immunodetection and fluorimetric visualization.

Quartz crystal microbalance

The binding affinity of Tau for Hsp90 was determined by QCM experiments using a low nonspecific binding quartz crystal chip coated with recombinant Hsp90 by amine coupling. Tau was injected in duplicate in seven concentrations ranging from 1 to 80 µg/ml on the Hsp90-coated chip and an empty crystal for the reference. All experimental details, a description of the data analysis procedures, simulations, and corresponding control experiments can be found in the Supplementary Materials.

SUPPLEMENTARY MATERIALS

Supplementary material for this article is available at http://advances.sciencemag.org/cgi/content/full/6/11/eaax6999/DC1

Supplementary Materials and Methods
Fig. S1. SDS gels of spin-labeled Tau.
Fig. S2. Mass spectrometry of spin-labeled Tau.
Fig. S3. Circular dichroism spectra of Tau.
Fig. S4. DEER data.
Fig. S5. RC model.
Fig. S6. Solvent-dependent RC model.
Fig. S7. Δ_{eff} as a measure for spin-spin separation.
Fig. S8. DEER data evaluation with different background corrections for doubly spin-labeled Tau.
Fig. S9. cw EPR data.
Fig. S10. QCM measurements.
Fig. S11. DEER data recorded in the presence of GdnHCl.
Table S1. Simulation of circular dichroism spectra.
Table S2. Kinetic analysis of QCM measurements.
Table S3. Overview of Δ_{eff} values and corresponding uncertainties (where applicable) as determined from various background analyses.
References (59–62)

View/request a protocol for this paper from *Bio-protocol*.

REFERENCES AND NOTES

1. E. M. Mandelkow, E. Mandelkow, Biochemistry and cell biology of tau protein in neurofibrillary degeneration. *Cold Spring Harb. Perspect. Med.* **2**, a006247 (2012).
2. Y. Wang, E. Mandelkow, Tau in physiology and pathology. *Nat. Rev. Neurosci.* **17**, 5–21 (2016).
3. E. H. Kellogg, N. M. A. Hejab, S. Poepsel, K. H. Downing, F. DiMaio, E. Nogales, Near-atomic model of microtubule-tau interactions. *Science* **360**, 1242–1246 (2018).
4. M. Goedert, Alzheimer's and Parkinson's diseases: The prion concept in relation to assembled Aβ, tau, and α-synuclein. *Science* **349**, 1255555 (2015).
5. T. Guo, W. Noble, D. P. Hanger, Roles of tau protein in health and disease. *Acta Neuropathol.* **133**, 665–704 (2017).
6. T. Crowther, M. Goedert, C. M. Wischik, The repeat region of microtubule-associated protein tau forms part of the core of the paired helical filament of Alzheimer's disease. *Ann. Med.* **21**, 127–132 (1989).
7. S. Jeganathan, M. von Bergen, H. Brutlach, H.-J. Steinhoff, E. Mandelkow, Global hairpin folding of tau in solution. *Biochemistry* **45**, 2283–2293 (2006).
8. M. D. Mukrasch, S. Bibow, J. Korukottu, S. Jeganathan, J. Biernat, C. Griesinger, E. Mandelkow, M. Zweckstetter, Structural polymorphism of 441-residue tau at single residue resolution. *PLOS Biol.* **7**, e1000034 (2009).
9. C. M. Wischik, M. Novak, P. C. Edwards, A. Klug, W. Tichelaar, R. A. Crowther, Structural characterization of the core of the paired helical filament of Alzheimer disease. *Proc. Natl. Acad. Sci. U.S.A.* **85**, 4884–4888 (1998).
10. S. Wegmann, I. D. Medalsy, E. Mandelkow, D. J. Müller, The fuzzy coat of pathological human tau fibrils is a two-layered polyelectrolyte brush. *Proc. Natl. Acad. Sci. U.S.A.* **110**, E313–E321 (2013).
11. A. W. P. Fitzpatrick, B. Falcon, S. He, A. G. Murzin, G. Murshudov, H. J. Garringer, R. A. Crowther, B. Ghetti, M. Goedert, S. H. W. Scheres, Cryo-EM structures of tau filaments from Alzheimer's disease. *Nature* **547**, 185–190 (2017).
12. B. Falcon, W. Zhang, A. G. Murzin, G. Murshudov, H. J. Garringer, R. Vidal, R. A. Crowther, B. Ghetti, S. H. W. Scheres, M. Goedert, Structures of filaments from Pick's disease reveal a novel tau protein fold. *Nature* **561**, 137–140 (2018).
13. C. A. Lasagna-Reeves, D. L. Castillo-Carranza, U. Sengupta, J. Sarmiento, J. Troncoso, G. R. Jackson, R. Kayed, Identification of oligomers at early stages of tau aggregation in Alzheimer's disease. *FASEB J.* **26**, 1946–1959 (2012).
14. C. A. Lasagna-Reeves, D. L. Castillo-Carranza, U. Sengupta, A. L. Clos, G. R. Jackson, R. Kayed, Tau oligomers impair memory and induce synaptic and mitochondrial dysfunction in wild-type mice. *Mol. Neurodegener.* **6**, 39 (2011).
15. F. Clavaguera, T. Bolmont, R. A. Crowther, D. Abramowski, S. Frank, A. Probst, G. Fraser, A. K. Stalder, M. Beibel, M. Staufenbiel, M. Jucker, M. Goedert, M. Tolnay, Transmission and spreading of tauopathy in transgenic mouse brain. *Nat. Cell Biol.* **11**, 909–913 (2009).
16. L. Liu, V. Drouet, J. W. Wu, M. P. Witter, S. A. Small, C. Clelland, K. Duff, Trans-synaptic spread of tau pathology in vivo. *PLOS ONE* **7**, e31302 (2012).
17. F. U. Hartl, A. Bracher, M. Hayer-Hartl, Molecular chaperones in protein folding and proteostasis. *Nature* **475**, 324–332 (2011).
18. F. H. Schopf, M. M. Biebl, J. Buchner, The HSP90 chaperone machinery. *Nat. Rev. Mol. Cell Biol.* **18**, 345–360 (2017).
19. F. Dou, W. J. Netzer, K. Tanemura, F. Li, F. Ulrich Hartl, A. Takashima, G. K. Gouras, P. Greengard, H. Xu, Chaperones increase association of tau protein with microtubules. *Proc. Natl. Acad. Sci. U.S.A.* **100**, 721–726 (2003).
20. C. A. Dickey, A. Kamal, K. Lundgren, N. Klosak, R. M. Bailey, J. Dunmore, P. Ash, S. Shoraka, J. Zlatkovic, C. B. Eckman, C. Patterson, D. W. Dickson, N. S. Nahman Jr., M. Hutton, F. Burrows, L. Petrucelli, The high-affinity HSP90-CHIP complex recognizes and selectively degrades phosphorylated tau client proteins. *J. Clin. Invest.* **117**, 648–658 (2007).
21. A. D. Thompson, K. M. Scaglione, J. Prensner, A. T. Gillies, A. Chinnaiyan, H. L. Paulson, U. K. Jinwal, C. A. Dickey, J. E. Gestwicki, Analysis of the tau-associated proteome reveals that exchange of Hsp70 for Hsp90 is involved in tau degradation. *ACS Chem. Biol.* **7**, 1677–1686 (2012).
22. E. Tortosa, I. Santa-Maria, F. Moreno, F. Lim, M. Perez, J. Avila, Binding of Hsp90 to tau promotes a conformational change and aggregation of tau protein. *J. Alzheimers Dis.* **17**, 319–325 (2009).
23. L. J. Blair, B. A. Nordhues, S. E. Hill, K. M. Scaglione, J. C. O'Leary III, S. N. Fontaine, L. Breydo, B. Zhang, P. Li, L. Wang, C. Cotman, H. L. Paulson, M. Muschol, V. N. Uversky, T. Klengel, E. B. Binder, R. Kayed, T. E. Golde, N. Berchtold, C. A. Dickey, Accelerated neurodegeneration through chaperone-mediated oligomerization of tau. *J. Clin. Invest.* **123**, 4158–4169 (2013).
24. L. B. Shelton, J. D. Baker, D. Zheng, L. E. Sullivan, P. K. Solanki, J. M. Webster, Z. Sun, J. J. Sabbagh, B. A. Nordhues, S. Koren III, S. Ghosh, B. S. J. Blagg, L. J. Blair, C. A. Dickey, Hsp90 activator Aha1 drives production of pathological tau aggregates. *Proc. Natl. Acad. Sci. U.S.A.* **114**, 9707–9712 (2017).
25. G. E. Karagöz, A. M. S. Duarte, E. Akoury, H. Ippel, J. Biernat, T. M. Luengo, M. Radli, T. Didenko, B. A. Nordhues, D. B. Veprintsev, C. A. Dickey, E. Mandelkow, M. Zweckstetter, R. Boelens, T. Madl, S. G. D. Rüdiger, Hsp90-Tau complex reveals molecular basis for specificity in chaperone action. *Cell* **156**, 963–974 (2014).
26. A. Pavlova, C.-Y. Cheng, M. Kinnebrew, J. Lew, F. W. Dahlquist, S. Han, Protein structural and surface water rearrangement constitute major events in the earliest aggregation stages of tau. *Proc. Natl. Acad. Sci. U.S.A.* **113**, E127–E136 (2016).
27. F.-X. Theillet, A. Binolfi, B. Bekei, A. Martorana, H. M. Rose, M. Stuiver, S. Verzini, D. Lorenz, M. van Rossum, D. Goldfarb, P. Selenko, Structural disorder of monomeric α-synuclein persists in mammalian cells. *Nature* **530**, 45–50 (2016).
28. M. Robotta, J. Cattani, J. C. Martins, V. Subramaniam, M. Drescher, Alpha-synuclein disease mutations are structurally defective and locally affect membrane binding. *J. Am. Chem. Soc.* **139**, 4254–4257 (2017).
29. Y. Fichou, M. Vigers, A. K. Goring, N. A. Eschmann, S. Han, Heparin-induced tau filaments are structurally heterogeneous and differ from Alzheimer's disease filaments. *Chem. Commun.* **54**, 4573–4576 (2018).
30. N. Le Breton, M. Martinho, E. Mileo, E. Etienne, G. Gerbaud, B. Guigliarelli, V. Belle, Exploring intrinsically disordered proteins using site-directed spin labeling electron paramagnetic resonance spectroscopy. *Front. Mol. Biosci.* **2**, 21 (2015).
31. S. Weickert, J. Cattani, M. Drescher, in *Electron Paramagnetic Resonance: Volume 26* (The Royal Society of Chemistry, 2019), vol. 26, pp. 1–37.
32. W. L. Hubbell, D. S. Cafiso, C. Altenbach, Identifying conformational changes with site-directed spin labeling. *Nat. Struct. Biol.* **7**, 735–739 (2000).
33. A. Milov, A. Ponomarev, Y. D. Tsvetkov, Electron-electron double resonance in electron spin echo: Model biradical systems and the sensitized photolysis of decalin. *Chem. Phys. Lett.* **110**, 67–72 (1984).
34. M. Pannier, S. Veit, A. Godt, G. Jeschke, H. W. Spiess, Dead-time free measurement of dipole–dipole interactions between electron spins. *J. Magn. Reson.* **213**, 316–325 (2011).
35. G. Jeschke, DEER distance measurements on proteins. *Annu. Rev. Phys. Chem.* **63**, 419–446 (2012).

36. D. Kurzbach, G. Platzer, T. C. Schwarz, M. A. Henen, R. Konrat, D. Hinderberger, Cooperative unfolding of compact conformations of the intrinsically disordered protein osteopontin. *Biochemistry* **52**, 5167–5175 (2013).

37. D. Kurzbach, T. C. Schwarz, G. Platzer, S. Höfler, D. Hinderberger, R. Konrat, Compensatory adaptations of structural dynamics in an intrinsically disordered protein complex. *Angew. Chem. Int. Ed.* **53**, 3840–3843 (2014).

38. A. M. Melo, J. Coraor, G. Alpha-Cobb, S. Elbaum-Garfinkle, A. Nath, E. Rhoades, A functional role for intrinsic disorder in the tau-tubulin complex. *Proc. Natl. Acad. Sci. U.S.A.* **113**, 14336–14341 (2016).

39. S. Elbaum-Garfinkle, E. Rhoades, Identification of an aggregation-prone structure of tau. *J. Am. Chem. Soc.* **134**, 16607–16613 (2012).

40. N. C. Fitzkee, G. D. Rose, Reassessing random-coil statistics in unfolded proteins. *Proc. Natl. Acad. Sci. U.S.A.* **101**, 12497–12502 (2004).

41. J. E. Kohn, I. S. Millett, J. Jacob, B. Zagrovic, T. M. Dillon, N. Cingel, R. S. Dothager, S. Seifert, P. Thiyagarajan, T. R. Sosnick, M. Z. Hasan, V. S. Pande, I. Ruczinski, S. Doniach, K. W. Plaxco, Random-coil behavior and the dimensions of chemically unfolded proteins. *Proc. Natl. Acad. Sci. U.S.A.* **101**, 12491–12496 (2004).

42. D. Chen, K. W. Drombosky, Z. Hou, L. Sari, O. M. Kashmer, B. D. Ryder, V. A. Perez, D. R. Woodard, M. M. Lin, M. I. Diamond, L. A. Joachimiak, Tau local structure shields an amyloid-forming motif and controls aggregation propensity. *Nat. Commun.* **10**, 2493 (2019).

43. L. Ferrari, R. Stucchi, A. Konstantoulea, G. van de Kamp, R. Kos, W. J. C. Geerts, F. G. Förster, M. A. F. Altelaar, C. C. Hoogenraad, S. G. D. Rüdiger, Fibril formation rewires interactome of the Alzheimer protein tau by π-stacking. *bioRxiv* **2019**, 522284 (2019).

44. J. R. Perkins, I. Diboun, B. H. Dessailly, J. G. Lees, C. Orengo, Transient protein-protein interactions: Structural, functional, and network properties. *Structure* **18**, 1233–1243 (2010).

45. S. Barghorn, E. Mandelkow, Toward a unified scheme for the aggregation of tau into Alzheimer paired helical filaments. *Biochemistry* **41**, 14885–14896 (2002).

46. N. D. Keul, K. Oruganty, E. T. Schaper Bergman, N. R. Beattie, W. E. McDonald, R. Kadirvelraj, M. L. Gross, R. S. Phillips, S. C. Harvey, Z. A. Wood, The entropic force generated by intrinsically disordered segments tunes protein function. *Nature* **563**, 584–588 (2018).

47. R. Sharma, Z. Raduly, M. Miskei, M. Fuxreiter, Fuzzy complexes: Specific binding without complete folding. *FEBS Lett.* **589**, 2533–2542 (2015).

48. M. Fuxreiter, Fold or not to fold upon binding—Does it really matter? *Curr. Opin. Struct. Biol.* **54**, 19–25 (2019).

49. J. Oroz, B. J. Chang, P. Wysoczanski, C.-T. Lee, Á. Pérez-Lara, P. Chakraborty, R. V. Hofele, J. D. Baker, L. J. Blair, J. Biernat, H. Urlaub, E. Mandelkow, C. A. Dickey, M. Zweckstetter, Structure and pro-toxic mechanism of the human Hsp90/PPIase/tau complex. *Nat. Commun.* **9**, 4532 (2018).

50. M. Radli, S. G. D. Rüdiger, Dancing with the Diva: Hsp90-client interactions. *J. Mol. Biol.* **430**, 3029–3040 (2018).

51. M. Taipale, D. F. Jarosz, S. Lindquist, HSP90 at the hub of protein homeostasis: Emerging mechanistic insights. *Nat. Rev. Mol. Cell Biol.* **11**, 515–528 (2010).

52. H. Kadavath, R. V. Hofele, J. Biernat, S. Kumar, K. Tepper, H. Urlaub, E. Mandelkow, M. Zweckstetter, Tau stabilizes microtubules by binding at the interface between tubulin heterodimers. *Proc. Natl. Acad. Sci. U.S.A.* **112**, 7501–7506 (2015).

53. M. Martinho, D. Allegro, I. Huvent, C. Chabaud, E. Etienne, H. Kovacic, B. Guigliarelli, V. Peyrot, I. Landrieu, V. Belle, P. Barbier, Two tau binding sites on tubulin revealed by thiol-disulfide exchanges. *Sci. Rep.* **8**, 13846 (2018).

54. D. Fischer, M. D. Mukrasch, J. Biernat, S. Bibow, M. Blackledge, C. Griesinger, E. Mandelkow, M. Zweckstetter, Conformational changes specific for pseudophosphorylation at serine 262 selectively impair binding of tau to microtubules. *Biochemistry* **48**, 10047–10055 (2009).

55. L. Ferrari, S. G. D. Rüdiger, Recombinant production and purification of the human protein Tau. *Protein Eng. Des. Sel.* **31**, 447–455 (2018).

56. Y. Motozato, T. Nishihara, C. Hirayama, Y. Furuya, Y. Kosugi, Competitive inclusion of chloro-substituted acetic acids into β-cyclodextrin monitored by rotational correlation frequencies of 4-hydroxy-2,2,6,6-tetramethylpiperidinyl-1-oxy radical. *Can. J. Chem.* **60**, 1959–1961 (1982).

57. R. A. Stein, A. H. Beth, E. J. Hustedt, in *Methods Enzymol,* Z. Q. Peter, W. Kurt, Eds. (Academic Press, 2015), vol. 563, pp. 531–567.

58. S. Brandon, A. H. Beth, E. J. Hustedt, The global analysis of DEER data. *J. Magn. Reson.* **218**, 93–104 (2012).

59. S. Barghorn, P. Davies, E. Mandelkow, Tau paired helical filaments from Alzheimer's disease brain and assembled in vitro are based on β-structure in the core domain. *Biochemistry* **43**, 1694–1703 (2004).

60. H. H. J. de Jongh, E. Goormaghtigh, J. A. Killian, Analysis of circular dichroism spectra of oriented protein-lipid complexes: Toward a general application. *Biochemistry* **33**, 14521–14528 (1994).

61. K. Krämer, *Physikalische Grundlagen der Maßeinheiten: Mit Einem Anhang über Fehlerrechnung* (Springer-Verlag, 2013).

62. G. Jeschke, V. Chechik, P. Ionita, A. Godt, H. Zimmermann, J. Banham, C. R. Timmel, D. Hilger, H. Jung, DeerAnalysis2006—A comprehensive software package for analyzing pulsed ELDOR data. *Appl. Magn. Reson.* **30**, 473–498 (2006).

Citation: S. Weickert, M. Wawrzyniuk, L. H. John, S. G. D. Rüdiger, M. Drescher, The mechanism of Hsp90-induced oligomerizaton of Tau. *Sci. Adv.* **6**, eaax6999 (2020).

Science Advances

The mechanism of Hsp90-induced oligomerizaton of Tau

S. WeickertM. WawrzyniukL. H. JohnS. G. D. RüdigerM. Drescher

View the article online
https://www.science.org/doi/10.1126/sciadv.aax6999
Permissions
https://www.science.org/help/reprints-and-permissions

Use of this article is subject to the Terms of service